

Trimethylsilyl-substituted ligands as solubilizers of metal complexes in supercritical carbon dioxide

Francisco Montilla,*†^a Vitor Rosa,^a Chris Prevett,^a Teresa Avilés,^a Manuel Nunes da Ponte,^a Dante Masi^b and Carlo Mealli^b

^a Departamento de Química, Centro de Química Fina e Biotecnologia, Faculdade de Ciências e Tecnologia, Universidade Nova de Lisboa, 2829-516 Caparica, Portugal

^b ICCOM, CNR, Via Nardi 39, 50132 Firenze, Italy

Received 17th December 2002, Accepted 26th March 2003

First published as an Advance Article on the web 10th April 2003

The SiMe₃ group (TMS), introduced as a substituent at the cyclopentadienyl ligand, is found to magnify the solubility of the corresponding metal complexes in supercritical carbon dioxide (scCO₂). This is verified from comparative solubility measurements of the species (η^5 -Me₃SiC₅H₄)MoO₂Cl, **1a**, (η^5 -Me₃SiC₅H₄)₂ZrCl₂, **2a**, and (η^5 -Me₃SiC₅H₄)Co(CO)I₂·0.5(I₂), **3a** (newly synthesised), and of their unsubstituted precursors **1b–3b**, respectively. In spite of the increased solubility, the chemical, structural and reactivity properties of the TMS derivatives are scarcely affected. Confirmation comes from a detailed study of the cobalt complex **3a** that includes X-ray structural determination. The geometry is most similar to that of the precursor **3b** while an apparently different Co–CO interaction is observed in the carboxylated analogue [(η^5 -PhCH₂CO₂C₅H₄)Co(CO)I₂, **3c**]. The problem is computationally tackled by using the DFT B3LYP method. The optimised geometries of the simplified models of **3a–3c** are all very similar. In particular, the computed stretching frequency of the unique CO ligand is consistent with the insignificant influence of the TMS group while it suggests a reduced amount of metal back-donation in **3c**. It is inferred that the TMS complexes **1a–3a**, while having higher solubility in scCO₂, maintain almost unaltered the electronic and chemical features of their parent compounds. In particular, the role of **1a–3a** as catalysts, that is well documented for homogeneous solutions, remains unaltered in the very different scCO₂ environment. The assumption is experimentally validated for **1a** by performing with the latter two classic catalytic processes. The first process is the oxidation of PPh₃ that is achieved by using molecular oxygen as an oxidant. The second example concerns the epoxidation of cyclohexene achieved in presence of *tert*-butyl hydroperoxide (TBHP).

Supercritical carbon dioxide (scCO₂) is becoming increasingly important as an alternative reaction medium to environmentally unfriendly organic solvents. CO₂ is non-toxic, relatively cheap, non-flammable and presents moderate critical constants ($T_c = 31.06$ °C, $P_c = 73.825$ bar). The tuning of the scCO₂ solvent capabilities has important potentialities such as a subtle control over the reactions, higher selectivities, improved reaction rates, *etc.* Moreover, the separation by simple decompression of reactants, catalyst and products becomes easier after the reaction.¹ These properties make scCO₂ a solvent that can potentially replace some of the conventional organic solvents in different applications such as homogeneous catalysis.²

The low solubility of many catalysts is usually an obstacle to their exploitation in scCO₂ homogeneously catalysed processes. The potentialities of scCO₂ as a solvent are comparable to those of saturated hydrocarbons. Consequently, the choice of the metal complex catalyst is considerably limited. Solubility studies of organometallic and coordination metal complexes have elucidated the factors that favour the solubility of a given catalyst in scCO₂.¹ These can be summarised as follows: the complexes should be non-polar, uncharged and hydrophobic. For example, the usage of ligands containing CO₂-philic moieties (*i.e.* perfluorinated alkyl groups, fluoroethers or alkyl siloxanes)³ has significantly increased in the last few years. Fluoroalkyl chains, directly fixed to some classic ligands, have permitted the design of new homogeneous catalysts, analogous to the conventional ones and they have been successfully employed in some important catalytic processes carried out in scCO₂.⁴ A possible drawback to their more generalized usage is the strong electron-withdrawing properties of the fluoroalkyl groups that affect the reactivity of the catalyst.⁵ A successful

solution to the latter problem has been found by using an appropriate spacer.^{4,6} In any case, the synthesis of ligands of this sort, as well as of their metal complexes, is usually difficult and expensive. For these reasons, the design of new solubilizers, that are easy to prepare but do not alter the chemical properties of the catalyst, is a highly desirable target.

We report here a new methodology to increase the solubility of cyclopentadienyl ligands and of their metal complexes in scCO₂. Thus, the functionalization of Cp with one trimethylsilyl (TMS) group has been attempted for different complexes of molybdenum, zirconium and cobalt. The solubility and properties of the newly synthesized compounds are compared with those of the parent, unsubstituted, precursors. In particular, the cobalt complex (η^5 -Me₃SiC₅H₄)Co(CO)I₂·0.5(I₂), **3a**, has been prepared for the first time and characterized by an X-ray structural analysis. Then, its structural features have been compared in detail with those available for other substituted and unsubstituted analogues. Further information has been derived from a series of DFT calculations that have been helpfully employed to compare the electronic effects attributable to the different substituents at the Cp ligand. Finally, with the purpose of verifying how the functionalisation of the Cp ligand may affect catalytic processes in scCO₂, we have used the molybdenum complex (η^5 -Me₃SiC₅H₄)MoO₂Cl, **1a**, to compare both the oxidation of PPh₃ by molecular oxygen and the epoxidation of cyclohexene by *tert*-butyl hydroperoxide (TBHP) in the different media.

Experimental

Infrared spectra were recorded as mulls on NaCl plates using an ATI Mattson Genesis FTIR spectrometer. Elemental analyses were performed at the microanalytical laboratory of the Universidade Técnica de Lisboa, Portugal. ¹H, ¹³C and ³¹P

† Present address: Departamento de Química Inorgánica, Universidad de Sevilla. Apto 553. 41071 Sevilla, Spain. E-mail: montilla@us.es

Table 1 Crystal data and structure refinement parameters for (η^5 -Me₃SiC₅H₄)Co(CO)₂·0.5(I₂) **3a**

Empirical formula	C ₉ H ₁₃ CoI ₃ OSi
Formula weight	604.91
Temperature/K	293(2)
$\lambda/\text{\AA}$	0.71073
Crystal system	Triclinic
Space group	P1
Unit cell dimensions	
$a/\text{\AA}$	6.720(3)
$b/\text{\AA}$	9.2099(11)
$c/\text{\AA}$	13.7765(10)
$\alpha/^\circ$	88.762(8)
$\beta/^\circ$	85.443(15)
$\gamma/^\circ$	71.088(17)
$V/\text{\AA}^3$	804.1(4)
Z	2
$D_s/\text{g cm}^{-3}$	2.498
μ/mm^{-1}	6.878
Unique reflections, $I > 2\sigma(I)$	2503
Final R indices [$I > 2\sigma(I)$]	R1 = 0.0324, wR2 = 0.0872
Final R indices (all data)	R1 = 0.0397, wR2 = 0.0912

NMR spectra were recorded on a Bruker ARX 400 spectrophotometer. ¹H NMR spectra were recorded using TMS as internal reference and ¹³C NMR spectra were referenced using the ¹³C resonance of the solvent as internal standard. ³¹P shifts were measured with respect to external 85% H₃PO₄. All reactions and manipulations of solutions were performed under an argon atmosphere using Schlenk techniques. Solvents were reagent grade and were dried according to literature methods. Triphenylphosphine, cyclohexene and TBHP (5.0–6.0 M solution in decane) were purchased from Aldrich and they were used as supplied. Na(η^5 -Me₃SiC₅H₄), (η^5 -Me₃SiC₅H₄)-MoO₂Cl **1a**,⁷ (η^5 -C₅H₅)MoO₂Cl **1b**,⁸ (η^5 -Me₃SiC₅H₄)₂ZrCl₂ **2a**,⁹ (η^5 -C₅H₅)₂ZrCl₂ **2b**,¹⁰ (η^5 -C₅H₅)Co(CO)₂ **3b**,¹¹ and (η^5 -Me₃-SiC₅H₄)Co(CO)₂,¹² were prepared according to the literature.

(η^5 -Me₃SiC₅H₄)Co(CO)₂·0.5(I₂) **3a**

Iodine (0.5 g, 2.0 mmol) was added at r.t. in portions to a stirred solution of (η^5 -Me₃SiC₅H₄)Co(CO)₂ (0.5 g, 2.0 mmol) in 50 ml of dry diethyl ether. The formation of a dark precipitate occurred immediately with simultaneous gas evolution. After stirring for 24 h at r.t., the solvent was partially removed under reduced pressure. Filtration of the solution and cooling to –20 °C afforded dark purple crystals of compound **3a** (820 mg, 40%).

¹H NMR (Cl₃CD): δ 5.96, 5.62 (s, 2, Cp), 0.45 (s, 9, Si(CH₃)₃). ¹³C{¹H} NMR (Cl₃CD): δ 207.03 (s, CO), 96.13, 92.85 (s, Cp), –0.49 (s, Si(CH₃)₃). C₉H₁₃CoSiI₃ (604.9): calc. C 17.85, H 2.15; found C 18.16, H 2.13%.

Crystallography. A summary of crystal and refinement data for **3a** is given in Table 1. A well-formed (dark purple) crystal was mounted on a Enraf-Nonius CAD4 diffractometer equipped with a graphite monochromator and Mo-K α radiation ($\lambda = 0.71073$ Å). Cell dimensions were refined by least-squares refinement of 25 reflections in the 2θ range 10–20°. During data collection, three standard reflections were monitored every two hours and insignificant decay was observed. The intensity data were corrected for Lorentz and polarization effects. Also the data were corrected for absorption by adopting the ψ -scan technique, T_{\max} and T_{\min} being evaluated as 0.23 and 0.30, respectively. Structure solutions were carried out by direct methods using the SIR97 package of programs.¹³ Refinements were made by full matrix least squares on all F^2 data using SHELXL97,¹⁴ with the scattering factors (f_o , f' and f'') using those described in the technical manual of the package. The hydrogen atoms bound to carbon atoms were introduced at calculated positions (C–H = 0.95 Å) in the later stages of refinement of ΔF maps. The anisotropic model was used for

the non-hydrogen atoms while the H atoms were treated with the riding model. No unusual trend in ΔF vs. F_o or $(\sin \theta)/\lambda$ was observed at the end of the refinement. Final difference syntheses showed no significant electron density residues. The molecular drawings were made by using the program ORTEP-III for Windows.¹⁵ All the computational work was performed by using the user-friendly graphic interface of WINGX.¹⁶

CCDC reference number 200044.

See <http://www.rsc.org/suppdata/dt/b2/b212386j/> for crystallographic data in CIF or other electronic format.

Computational details. Geometry optimisations of the model compounds (η^5 -RC₅H₄)Co(CO)Cl₂ (R = H, SiH₃, CO₂H) were carried out within the density functional theory. In all cases, the hybrid B3LYP functional was used¹⁷ with the basis set 6-31G(d,p) for all of the atoms. The effective core potential (LANL2DZ) was used for cobalt.¹⁸ The optimised geometries were characterized as local energy minima by diagonalisation of the analytically computed Hessian. The systematic calculation of the normal modes of vibrations (frequencies) is also a major strategy to evaluate the electronic effects introduced at the metal by the different substituent at the Cp ring. All the calculations were performed by using the Gaussian 98 suite of programs.¹⁹

Experiments in supercritical CO₂. A simple high-pressure apparatus, described elsewhere,²⁰ was used to carry out the solubility measurements and the reactions in scCO₂. Two view cells, with volumes of 4 and 11 ml and equipped with sapphire windows were used for the experiments. A schematic diagram of the apparatus is shown in Fig. 1.

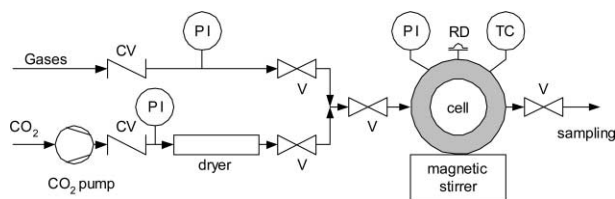


Fig. 1 Schematic diagram of the apparatus. TC: Temperature controller, PI: Pressure indicator, V: Valve, CV: Non-return valve, RD: Rupture disk.

Catalysts and reagents were inserted into the cell under argon, the reactor evacuated, and then refilled with argon. The cell was subsequently placed in the high-pressure line. CO₂ (purity 99.9999% from Carbueros Metálicos) was transferred into the cell by using a pneumatic liquid pump. The cell was heated to the desired temperature in a water bath. A digital transducer was used to measure the pressure. In order to reach complete homogeneity of the solution by stirring, the cell must be suitably placed at the bottom of the water bath as close as possible to the stir plate. Care must be taken to avoid irregular movements of the magnetic Teflon bar. After each experiment, the cell was carefully depressurised at 0 °C through an ethanol trap.

Solubility measurements. For solubility measurements, a sufficient amount of compound was put into the view cell (11 ml), to give a saturated solution in scCO₂ at 40 °C and at the corresponding pressure. This was visually checked by the presence of the solid compound in the cell at the given pressure. Before performing any measurement, the mixtures were efficiently stirred for several hours in order to guarantee that saturation of the complex in the supercritical phase had been achieved. Samples were taken through a high-pressure sample loop (0.5 ml), by filling with the supercritical fluid mixture, depressurising into a sample vial, and flushing with Cl₂CH₂. Subsequently, the sample loop was dried with compressed air.

The concentrations of the Cl_2CH_2 solutions was determined by analysing them by UV spectroscopy. These experiments were performed for each compound at least three times and the final value was taken as the average of all of the measurements.

Oxidation of triphenylphosphine using O_2 in scCO_2 . A 21 : 1 mixture of PPh_3 (0.055 g, 0.21 mmol) and $(\eta^5\text{-Me}_3\text{SiC}_5\text{H}_4)\text{-MoO}_2\text{Cl}$ **1a** (0.0031 g, 0.01 mmol) was prepared as the supplied material. 0.0104 g of the latter was used for each experiment. The amount was charged into the 4-ml high-pressure cell. The cell was heated at 40 °C, then, molecular oxygen was added at the required pressure and, immediately, CO_2 was added using a pneumatic pump. The sapphire windows allowed confirmation of a single fluid phase and of complete dissolution of the reagent mixture. After reaction, CO_2 was slowly vented and the surplus was extracted with CH_2Cl_2 . Conversions to phosphine oxide were determined by ^{31}P NMR analysis (a deuterated benzene capillary was used as reference).

Kinetic studies in scCO_2 were achieved by repeating the experiments using identical conditions ($[\text{PPh}_3]_0 = 9.16 \text{ mmol L}^{-1}$, $P_{\text{O}_2} = 5 \text{ bar}$, $P_{\text{T}} = 180 \text{ bar}$) changing the reaction time. Pseudo-second-order conditions were employed ($[\text{substrate}] : [\text{Mo complex}] = 21 : 1$). Conversions were determined as above.

The 11-ml cell was used when dealing with the more conventional solvents. The reaction mixture used was prepared as before and it was charged in the high-pressure cell with 4 ml of the respective solvent. The cell was heated to 40 °C and O_2 (5 bar) added. After 1 h the cell was depressurised and the solvent removed. Conversions were established as above.

Oxidation of cyclohexene using TBHP in scCO_2 . In each experiment, the catalyst (0.0031 g, 0.01 mmol) was added to the high-pressure cell (11 ml) that hosted a small container of cyclohexane (0.058 g, 0.70 mmol) and TBHP solution (0.15 ml, *ca.* 0.80 mmol). Precaution was taken in order to avoid any direct reaction between the catalyst and the latter species prior to the introduction of CO_2 . The cell was heated to the desired temperature and then, charged with CO_2 . The sapphire windows confirmed the homogeneity of the reaction mixture. After the allotted reaction time, the cell was depressurised as previously described and the residue was extracted with CDCl_3 (containing 1% TMS) for NMR analysis. Conversions to cyclohexane oxide were determined by ^1H NMR analysis (TMS peak was used as internal reference).

Results and discussion

Solubility of cyclopentadienyl-complexes in scCO_2

The complexes $(\eta^5\text{-Me}_3\text{SiC}_5\text{H}_4)\text{MoO}_2\text{Cl}$, **1a**,⁷ $(\eta^5\text{-Me}_3\text{SiC}_5\text{H}_4)_2\text{-ZrCl}_2$, **2a**,⁹ together with the newly synthesized cobalt species $(\eta^5\text{-Me}_3\text{SiC}_5\text{H}_4)\text{Co}(\text{CO})\text{I}_2 \cdot 0.5(\text{I}_2)$, **3a**, have been used to study the solubilising effects of the TMS groups in scCO_2 . For comparison, the measurements were performed in parallel with those of the analogous non-substituted derivatives $(\eta^5\text{-C}_5\text{H}_5)\text{-MoO}_2\text{Cl}$ **1b**,⁸ $(\eta^5\text{-C}_5\text{H}_5)_2\text{ZrCl}_2$ **2b**,¹⁰ $(\eta^5\text{-C}_5\text{H}_5)\text{Co}(\text{CO})\text{I}_2$ **3b**.¹¹ In practice, a high-pressure sample loop, coupled to the high-pressure cell, was filled with the saturated supercritical fluid mixture. Subsequent depressurisation was produced into a sample vial and then, the loop was flushed with Cl_2CH_2 . UV spectroscopy analysis of the resulting solutions gave the concentration of the compounds in scCO_2 . Table 2 summarises the solubility values of **1a–3a** and **1b–3b** at 40 °C. In the case of molybdenum and zirconium, the solubility of the TMS-substituted species increased by a factor of three or four. In the case of cobalt, the increase of solubility was up to six times larger. It is worth stressing that the concentration ranges (1 mM or higher), that are generally adopted for homogeneous catalytic processes, was achieved also for the TMS-substituted complexes **1a–3a** solubilised in scCO_2 . Despite the enormous interest for homogeneous catalysis, operations with organo-

Table 2 Data for the solubility (40 °C) of cyclopentadienyl derivatives in scCO_2

Compound	Concentration/mol L ⁻¹	P/bar
$(\eta^5\text{-Me}_3\text{SiC}_5\text{H}_4)\text{MoO}_2\text{Cl}$ 1a	5.81×10^{-3}	102
$(\eta^5\text{-C}_5\text{H}_5)\text{MoO}_2\text{Cl}$ 1b	1.55×10^{-3}	128
$(\eta^5\text{-Me}_3\text{SiC}_5\text{H}_4)_2\text{ZrCl}_2$ 2a	1.38×10^{-3}	103
$(\eta^5\text{-C}_5\text{H}_5)_2\text{ZrCl}_2$ 2b	0.47×10^{-3}	104
$(\eta^5\text{-Me}_3\text{SiC}_5\text{H}_4)\text{Co}(\text{CO})\text{I}_2$ 3a	0.41×10^{-4}	99
$(\eta^5\text{-C}_5\text{H}_5)\text{Co}(\text{CO})\text{I}_2$ 3b	0.07×10^{-3}	95

Table 3 Infrared data on the π -cyclopentadienyl metal carbonyls

Compound	R = SiMe ₃	R = H
$(\eta^5\text{-C}_5\text{H}_4\text{R})\text{Mn}(\text{CO})_3$	2024, 1943 ^a	2026, 1935 ^b
$(\eta^5\text{-C}_5\text{H}_4\text{R})\text{Re}(\text{CO})_3$	2027, 1937 ^a	2041, 1939 ^c
$(\eta^5\text{-C}_5\text{H}_4\text{R})\text{Co}(\text{CO})_2$	2025, 1966 ^a	2024, 1963 ^d
$(\eta^5\text{-C}_5\text{H}_4\text{R})\text{Co}(\text{CO})\text{I}_2$	2065 ^e	2068 ^f

^a Solvent cyclohexane, ref. 12. ^b Solvent C_6H_6 , ref. 22. ^c Solvent CCl_4 , ref. 23. ^d Ref. 24. ^e Nujol. ^f Nujol, ref. 11.

metallic compounds dissolved in the latter medium are not so common.¹ There is evidence only for some classical complexes of the first-row transition metals, such as ferrocene and some of its derivatives, some metal chlorides and a range of metal carbonyls (*e.g.*, $\text{Co}_2[\text{CO}]_8$, $\text{Fe}[\text{CO}]_5$, $\text{CpCo}[\text{CO}]_2$).^{20a,21} Even more scarce is the number of second- and third-row metal compounds soluble in scCO_2 . These are generally limited to species containing fluorinated chains in the ligands.⁴ Thus, the different nature of the present molybdenum and zirconium complexes **1a** and **2a**, that have good solubility in scCO_2 , is particularly relevant.

Although the increase of solubility upon TMS-substitution appears smaller than that occurring when the unsubstituted precursor is fluorinated,^{4a} an important point to be made is that the introduction of the TMS group does not cause any major modification of the chemical properties at the metal with respect to the parent unsubstituted compound. In this respect, the CO stretching frequency can be used as a sensitive indicator of structural and electronic variations at the metal center. In the last row of Table 3, the comparative values relative to the complexes **3a** and **3b** indicate a minimum variation. This is true also for other pairs of complexes that differ only for the absence or presence of a TMS group at the cyclopentadienyl ring.^{12,22–24} The effects on the CO coligand are further elucidated from detailed comparisons between the experimental and calculated structural features of **3a**, **3b** and those of the carboxylated congener $(\eta^5\text{-PhCH}_2\text{CO}_2\text{C}_5\text{H}_4)\text{Co}(\text{CO})\text{I}_2$, **3c**,^{25a} (*vide infra*).

Molecular structure of **3a**

The structure of **3a** was determined by X-ray crystallography on crystals grown from a diethyl ether solution. The crystal lattice contains molecules of the $(\eta^5\text{-Me}_3\text{SiC}_5\text{H}_4)\text{Co}(\text{CO})\text{I}_2$ and of iodine in a ratio 2 : 1. Fig. 2 reports an ORTEP drawing that shows both units.

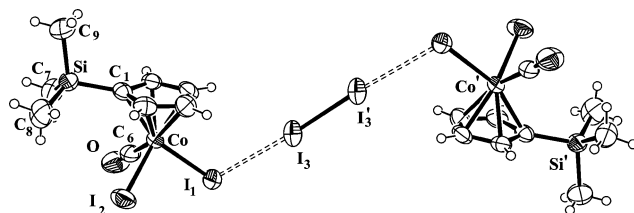


Fig. 2 ORTEP drawing illustrating two complex molecules of $(\eta^5\text{-Me}_3\text{SiC}_5\text{H}_4)\text{Co}(\text{CO})\text{I}_2$ and one interspersed iodine molecule sitting on a center of inversion. Weak acid–base interactions are formed by the latter diatomic and iodide ligands of the two complex molecules ($\text{I} \cdots \text{I}$ separation = 3.41(1) Å).

Table 4 Comparison between selected bond lengths (Å) and angles (°) in the present for the complex (η^5 -Me₃SiC₅H₄)Co(CO)I₂·0.5I₂ **3a** and in the parent complex (η^5 -C₅H₅)Co(CO)I₂ **3b**, and (η^5 -PhCH₂CO₂C₅H₄)Co(CO)I₂ **3c**

	3a	3b^a	3c^b
Co(1)–C(6)	1.781(7)	1.76(1)	1.865(6)
Co(1)–C(3)	2.067(6)	2.029(13)	2.073(6)
Co(1)–C(2)	2.066(6)	2.032(9)	2.054(6)
Co(1)–C(4)	2.076(6)	2.032(9)	2.064(6)
Co(1)–C(5)	2.089(6)	2.065(7)	2.081(6)
Co(1)–C(1)	2.099(6)	2.065(7)	2.053(6)
Co(1)–I(2)	2.568(9)	2.565(3)	2.557(1)
Co(1)–I(1)	2.580(9)	2.565(3)	2.558(1)
Si(1)–C(1)	1.873(6)		
C(7)–C(1)			1.462(9)
O(1)–C(6)	1.125(8)	1.13(1)	1.050(9)
I(3)–I(3')	2.736(1)		
C(6)–Co(1)–I(2)	88.8(2)	89.1(2)	87.9(2)
C(6)–Co(1)–I(1)	87.3(2)	89.1(2)	87.0(2)
I(2)–Co(1)–I(1)	93.81(3)	94.0(1)	94.0(5)
O(1)–C(6)–Co(1)	178.8(7)	179.4(1)	178.1(7)

^a Ref. 11c. ^b Ref. 25a.

The Co(III) complex has a typical three-legged piano stool structure. One of the coordinated iodine atoms, I(1), is involved in a weak donor–acceptor interaction with the I₂ molecule of crystallization. The latter lies on a center of inversion and is almost collinear with the intermolecular I(1)–I(3) vector [I(1)–I(3)–I(3') angle 176.0(3)°]. The bond distances and angles of **3a** can be conveniently compared with those of two strictly related compounds, **3b**^{11c} and **3c**,^{25a} available from the literature (see Table 4). In general, the angles at the metal and the Co–I distances are very similar in the three compounds while only the unsubstituted Cp rings shows the shortest Co–C distances. However, the most striking difference seems to affect the binding mode of the CO ligand in complex **3c**. In fact, the Co–C distance of 1.865(6) Å is about 0.1 Å longer than the corresponding average value for structures **3a** and **3b** (very similar between themselves). At the same time the C–O separation within the coordinated carbon monoxide molecule is unusually short in **3c** [1.05(1) Å vs. the average value of 1.1275(10) Å in **3a** and **3b**]. In this respect, it is useful to recall that distances between atoms affected by large temperature factors are usually underestimated (in **3c** the carbonyl oxygen atom has a *B*_{eq} temperature factor of 7.6 that is about 30–40% greater than that of any other non-hydrogen atom in the structure). The C–O distance appears definitely shorter than that in the free carbon monoxide (1.10 Å). This may occur in adducts of the non-classical type such as those formed by the electropositive metals Cu⁺ and Ag⁺,²⁶ but it cannot be the case here. Although the crystallographic result for **3c** is evidently suspicious, it may still be indicative of an almost null metal back-donation. In fact, a good π -acceptor group, such as the carboxylate substituent (almost coplanar with the Cp ring), has potential mesomeric capabilities. Thus an increased attraction of electron density toward Cp should diminish the back-donating power of the metal toward CO. In principle, also an electropositive atom such as silicon can produce such an effect but the Co–C distance is insignificantly larger in **3a** vs. **3b** (1.781(7) and 1.76(1) Å, respectively) and so is the shortening of the C–O distance (1.125(8) vs. 1.13(1) Å). These points will be further illustrated below where the results of DFT optimisations on models of **3a–3c** are presented.

A final remark about the structure of **3a** concerns the donor–acceptor aggregate between two complex units and one I₂ molecule. The situation is clearly highlighted in Fig. 2. On the basis of structural and spectroscopic features D·I₂ adducts (D = donor base) are classified into three groups, namely D···I–I, D–I–I and D–I⁺···I[–].²⁷ There is an inverse correlation

between the D–I and the I–I distances that depends on the donor capabilities of the base. One of us has recently contributed to a theoretical model that goes beyond the classic four electron–three center model as it considers the different contributions of as many as four orbitals and six electrons in the systems.²⁸ Obviously, the present case belongs to the first typology, with the intramolecular I(3)–I(3') distance of 2.736(1) Å being insignificantly elongated with respect to the bond length of the free I₂ molecule [2.715(1) Å] and the linear I···I–I interactions being quite elongated.

DFT calculations on the models (η^5 -RC₅H₄)Co(CO)Cl₂, R = H, SiH₃, CO₂H

Geometry optimisations at the B3LYP level with the 6-31G(d,p) basis set were carried out on simplified models (**3a'–3c'**) of the complexes **3a–3c**. The chloride ligands were selected to avoid the many-electron iodine element and the degree of uncertainties for its basis set. Also the simplest silyl substituent was used in place of the three-methyl one, that is present in **3a**, in order to reduce the complexity of the calculation. For the same reason CO₂H replaces in **3c'** the group CO₂CH₂Ph of **3c**. Since we are mainly interested in trends, the introduced simplifications should not obscure the basic electronic effects on the primary structure and on the metal–carbonyl interaction, in particular.

Fig. 3 shows the optimised structures **3a'–3c'** with selected bond distances and angles. Compared with the corresponding experimental structures (see Table 4), the results appear acceptably good. The backbones of the computed structures are quite similar to each other, only some asymmetry of the Co–C_{cp} distances being observed for the species **3c'**. The latter distances are generally longer than the experimental ones as well as the Co–C(O) distances, with the exception of **3c'** and **3c** where the order is reversed. This is true also for the C–O distances, thus indicating that the very small MCO back-donation, suggested by the experimental structure of **3c**, is not supported by the calculations. In actuality, the Co–C(O) and C–O bonds are pretty constant in the series **3a'–3c'**. A strategy to verify the extent of the back-donation in these compounds and their dependence on the nature of the substituents is to look at the normal modes of CO vibrations calculated for **3a'–3c'**. The CO stretching frequency of carbon monoxide (scaled by a factor of

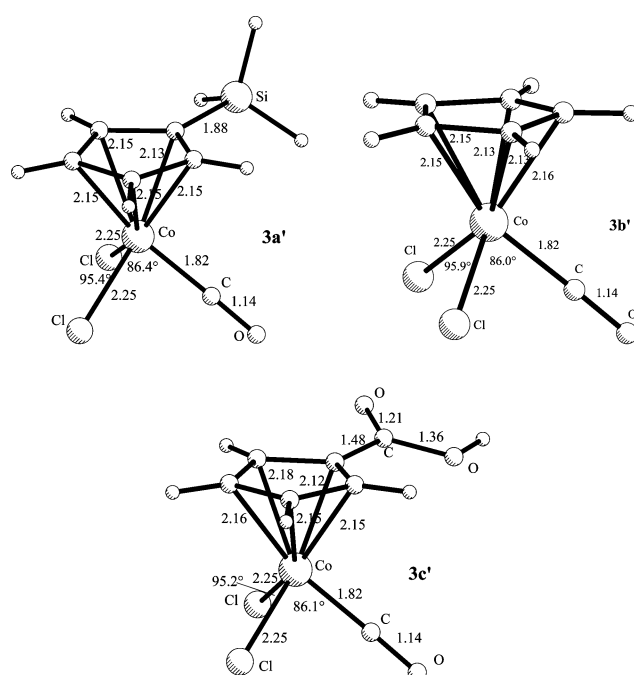


Fig. 3 B3LYP optimised structures of models of the complexes **3a**, **3b** and **3c**.

Table 5 Oxidation of PPh₃ by (η^5 -Me₃SiC₅H₄)MoO₂Cl **1a** using molecular oxygen^a

Entry	Solvent	PPh ₃ /catalyst ratio	P _{CO₂} /bar	P _{O₂} /bar	t/h	Conversion ^d (%)
1 ^b	scCO ₂	No catalyst	180	5	24	2
2 ^b	scCO ₂	21	180	5	24	100
3 ^b	scCO ₂	21	160	1	1	38
4 ^b	scCO ₂	21	160	2	1	42
5 ^b	scCO ₂	21	160	3	1	54
6 ^b	scCO ₂	21	160	5	1	63
7 ^c	Hexane	21	–	5	1	47
8 ^c	Toluene	21	–	5	1	63
9 ^c	CHCl ₃	21	–	5	1	76

^a [catalyst] = 0.45 mmol L⁻¹, [PPh₃] = 9.4 mmol L⁻¹. ^b V_{cell} = 4 ml. ^c V_{solvent} = 4 ml. ^d Conversion to triphenylphosphine oxide (calculated by ³¹P NMR).

0.96 adopted for B3LYP//6-31G(d,p) model chemistry²⁹ is computed to be 2107.3, 2107.9 and 2116.5 cm⁻¹ for **3a'**, **3b'** and **3c'**, respectively. The trend is fully consistent with the experimental values reported for **3a**, **3b**¹¹ and **3c**,^{23b} *i.e.* 2065, 2068 and 2073 cm⁻¹, respectively. This result confirms that the present species are not comparable with the metal–carbonyl complexes of the non-classical type for which the CO frequencies are 2143 cm⁻¹ or higher, as experimentally and theoretically reported.^{26,30} In conclusion, the carboxylate group is confirmed to reduce somewhat the back-donating capabilities of the metal in **3c**, whereas the silylated compound behaves practically as the parent one.

Catalytic processes in scCO₂

Oxidations carried out in scCO₂ as solvent medium have received significant attention in the last few years. These homogeneous systems are formed by a transition metal catalyst and O₂ or peroxides as oxidant.³¹ The latter processes offer several advantages such as (i) the exclusion of organic solvents and the usage of the more environmentally benign carbon dioxide in their place, (ii) the complete miscibility in scCO₂ of oxidants such as O₂ thus eliminating interphase transport limitations, (iii) the resistance of CO₂ to oxidation.

Here, we confirm the untouched potentialities of the TMS-substituted cyclopentadienyl complexes as catalysts when dissolved in scCO₂. In particular, we have selected the complex (η^5 -Me₃SiC₅H₄)MoO₂Cl, **1a**, to test the occurrence of two classic catalytic reactions. The first reaction concerns the oxidation of PPh₃ with molecular oxygen as oxidant. It should be stressed that activation of latter molecule is one of the great challenges for synthetic chemistry, in particular its application in the selective oxidation of hydrocarbons.³² Thus, the test appears important and appropriate to confirm the potentialities of **1a** as a catalyst in scCO₂.

The second test is also interesting because it concerns the important oxidation of stable organic substrates such as hydrocarbons. In particular, molybdenum complexes are known to catalyse the epoxidation of olefins by alkyl hydroperoxides,³³ and previous studies involving Cp*MoO₂Cl (Cp* = pentamethylcyclopentadienyl)³⁴ indicate that complex **1a** should be an ideal catalyst for these oxidations in scCO₂. Accordingly, we used again the latter to test the epoxidation of cyclohexene in presence of *tert*-butyl hydroperoxide (TBHP).

Oxidation of PPh₃ in scCO₂ in the presence of the catalyst (η^5 -Me₃SiC₅H₄)MoO₂Cl and molecular oxygen

Table 5 summarizes the significant results for the oxidation of PPh₃ under various conditions. Reactions were carried out in presence of **1a** in a PPh₃ : catalyst ratio of 21 : 1. In the reactions performed in scCO₂, both catalyst and phosphine were placed in a high pressure cell, charged with O₂ and then with CO₂ to the required pressure. In all cases, a fully homogenous single-phase was obtained. After the reaction, the cell was carefully vented and the residue was extracted with CH₂Cl₂.

Conversions to phosphine oxide were determined by ³¹P NMR analysis.

No significant quantities of the phosphine oxide were produced in the absence of the Mo complex (entry 1), while complete oxidation of PPh₃ was observed when the reaction was carried out in the presence of **1a** (entry 2). These results clearly showed the importance of the metal catalyst in the process. The noticeable increase in the conversion of PPh₃ with an increase of the oxygen partial pressure (entries 3–6) reveals the importance of this parameter. Finally, the effect of the solvent was analysed by comparing the reaction performed in four solvents with different chemical properties (entries 6–9). When the experiment was carried out in hexane, which resembles the behaviour of scCO₂,³⁵ the reaction was clearly slower than that carried out in scCO₂ under similar conditions. The result stresses the advantage of performing the reaction in scCO₂ with respect to conventional solvents as the solubility of oxygen in the supercritical solvent is definitely higher. When the reactions were performed in toluene or chloroform, that have a higher polarity than scCO₂, the observed conversions were similar and higher, respectively.

The kinetics of the process in scCO₂ was investigated. The disappearance of the ³¹P NMR band of PPh₃ was used to monitor the reaction. Plots of 1/[PPh₃] *vs.* time were linear indicating that the reaction was second order with respect to the phosphine concentration with $k_{\text{obs}} = 3.28 \times 10^{-2} \text{ mol}^{-1} \text{ L s}^{-1}$. The generally accepted mechanism for reactions of this type,³⁶ implies transfer of the oxygen atom from the [Mo^{VI}O₂]²⁺ center to the phosphine followed by an oxidation that regenerates the active site. A precise description of the reaction kinetics requires further experimental work that is already planned. Such a task is, however, beyond the immediate goal of this work.

Oxidation of cyclohexene using TBHP in scCO₂

Epoxidation of cyclohexene carried out with O₂ as oxidant failed under various conditions. Also, the tests with hydrogen peroxide as oxidant were predictably unsuccessful due to the formation of peroxy-complexes that remain completely inactive in processes of this sort.³⁴ Eventually, we successfully selected TBHP as the oxidant for our test catalysis.

Catalyst and reagents were placed separately into the high-pressure view cell in order to ensure that no reaction takes place until there is full homogeneity (*i.e.* until supercritical conditions are reached). Through the sapphire windows, the homogeneity of the reaction mixture could be confirmed. After the required reaction time, the cell was depressurised as previously described and the residue was extracted with CDCl₃. Conversions to cyclohexane oxide were determined by ¹H NMR analysis (Table 6).

As expected, complex **1a** was shown to be a good catalyst for this type of reaction in scCO₂. The conversion values found, however, are less satisfactory than those obtained by using a similar catalyst in conventional solvents.^{34a} This is likely the consequence of the difficulties in calculating the conversion

Table 6 Data for the oxidation of cyclohexene in scCO₂

Entry	t/h	^t BuOOH : cyclohexene : catalyst ratio	T/°C	Conversion ^a (%)
1	–	1 : 1 : 0 (no catalyst)	40	–
2	1	1 : 1 : 0.014	40	40
3	1	1 : 1 : 0.014	50	27
4	1	1 : 1 : 0.014	60	29
5	15	1 : 1 : 0.014	60	27
6	1	1 : 1 : 0.014	70	29

^a Conversion to cyclohexene oxide (calculated by ¹H NMR).

values. In fact, the use of cyclohexene as substrate was not found to be a good choice due to the low boiling point of the substrate and the product. In scCO₂ small losses of material occurred during the depressurisation process and accurate calculation of the conversion values is difficult.

Conclusions and extensions

The combined experimental and computational study supports the basic idea, that a good catalyst can function also in supercritical CO₂, provided that good solubility is achieved in the medium. We have found that transition metal catalysts with a cyclopentadienyl ligand are more easily dissolved in scCO₂ when a trimethylsilyl group is introduced at the Cp ligand. It must be pointed out, however, that the effect is not likely a consequence of the electropositive silicon atom of the TMS group but is in line with the general good solubility of saturated hydrocarbons in scCO₂. In other words, the study shows that the TMS group helps to solubilise a metal complex in scCO₂ but it does not alter the electronic properties of the metal center which maintains its functionality as a catalyst. Insignificant effects on the geometry were confirmed from the comparison of the crystal structures of three analogous complexes (η^5 -RC₅H₄)-Co(CO)₂L₂ as well as from that of their computationally optimised models. In particular, it is observed that some substituents (e.g., a carboxylate group) can affect the stretching frequency of the unique CO ligand, and hence the electronic distribution at the metal. Conversely, the silyl substituent leaves the back-donating power of the metal unaltered with the reactivity almost matching that of the parent unsubstituted compound.

Good solubility of a classical metal catalyst in scCO₂ is a prerequisite to carry out catalysis in this environment which differs significantly from that of homogeneous solutions. The feasibility of catalysis in scCO₂ is confirmed by two classic reactions, viz. the oxidation of PPh₃ and the epoxidation of cyclohexene. Presently, we are attempting to increase the solubility of selected catalysts in scCO₂ by introducing TMS substituents at some phosphine ligands. Importantly, the use of the latter in homogeneous catalysis is even more widespread than that of cyclopentadienyl ligands.

Acknowledgements

The authors acknowledge the financial support from Fundação para a Ciência e Tecnologia (Project PRAXIS/P/QUI/10075) and European Commission (Contracts FMRX-CT97-0104-DLCL) and HPMF-CT-1999-00373). This collaborative work has been also made possible thanks to the bilateral projects CNR-ICCTI, 2001-2002, (Italy-Portugal) and Accion Integrada HP2001-0066, (Spain-Portugal).

References

- (a) P. G. Jessop and W. Leitner, in *Chemical Synthesis Using Supercritical fluids*, Wiley-VCH, 1999; (b) *Supercritical Fluids*, *Chem. Rev.*, 1999, **99** (2).
- (a) R. J. Sowden, M. F. Sellin, N. De Blasio and D. J. Cole-Hamilton, *Chem. Commun.*, 1999, 2511; (b) C. A. G. Carter, R. T. Baker, S. P. Nolan and W. Tumas, *Chem. Commun.*, 2000, 347; (c) T. J. de Vries, R. Duchateau, M. A. G. Vorstman and J. T. F. Keurentjes, *Chem. Commun.*, 2000, 263.
- A. V. Yazdi and E. J. Beckman, *Ind. Eng. Chem. Res.*, 1996, **35**, 3644.
- (a) S. Kainz, D. Koch, W. Baumann and W. Leitner, *Angew. Chem., Int. Ed. Engl.*, 1997, **36**, 1628; (b) S. Kainz, A. Brinkmann, W. Leitner and A. Pfaltz, *J. Am. Chem. Soc.*, 1999, **121**, 6421; (c) M. Carroll and A. B. Holmes, *Chem. Commun.*, 1998, 1395; (d) T. Osswald, S. Schneider, S. Wang and W. Bannwarth, *Tetrahedron Lett.*, 2001, **42**, 2965.
- D. R. Palo and C. Erkey, *Organometallics*, 2000, **19**, 81.
- (a) B. Richter, A. L. Spek, G. Van-Koten and B. J. Deelman, *J. Am. Chem. Soc.*, 2000, **122**, 3945; (b) B. Richter, E. de Wolf, B. J. Deelman and G. Van-Koten, *J. Org. Chem.*, 2000, **65**, 3885.
- T. Robin, F. Montilla, A. Galindo, C. Ruiz and J. Hartmann, *Polyhedron*, 1999, **18**, 1485.
- M. Cousins and M. L. H. Green, *J. Chem. Soc. A*, 1964, 1567.
- M. F. Lappert, C. J. Pickett, P. I. Riley and P. I. W. Yarrow, *J. Chem. Soc., Dalton Trans.*, 1981, 805.
- E. Samuel, *Bull. Soc. Chim. Fr.*, 1966, 3548.
- (a) R. B. King, *Z. Naturforsch., Teil B*, 1964, **19**, 1160; (b) R. F. Heck, *Inorg. Chem.*, 1965, **4**, 855; (c) T. Avilés, A. Dinis, J. O. Gonçalves, V. Felix, M. J. Calhorda, A. Prazeres, M. G. B. Drew, H. Alves, R. T. Henriques, V. de Gama, P. Zanello and M. Fontani, *J. Chem. Soc., Dalton Trans.*, 2002, 4595.
- E. W. Abel and S. Moorhouse, *J. Organomet. Chem.*, 1971, **28**, 215.
- SIR97: A. Altomare, M. C. Burla, M. Cavalli, G. L. Casciarano, C. Giacovazzo, A. Gagliardi, A. G. G. Moliterni, G. Polidori and R. Spagna, *J. Appl. Crystallogr.*, 1999, **32**, 115.
- G. M. Sheldrick, SHELXL-97, Program for refinement of crystal structures, University of Göttingen, Germany, 1997.
- (a) ORTEP-III: M. N. Burnett, C. K. Johnson, Report ORNL-6895, Oak Ridge National Laboratory, Oak Ridge, TN, 1996; (b) L. J. Farrugia, *J. Appl. Crystallogr.*, 1997, **30**, 565.
- (a) L. J. Farrugia, *J. Appl. Crystallogr.*, 1999, **32**, 837.
- (a) A. D. Becke, *J. Chem. Phys.*, 1993, **98**, 5648; (b) C. Lee, W. Yang and R. G. Parr, *Phys. Rev. B*, 1988, **37**, 785.
- (a) T. H. Dunning, Jr. and P. J. Hay, *Modern Theoretical Chemistry*, Plenum, New York, 1976, p. 1; P. J. Hay and W. R. Wadt, *J. Chem. Phys.*, 1985, **82**, 299.
- M. J. Frisch, G. W. Trucks, H. B. Schlegel, G. E. Scuseria, M. A. Robb, J. R. Cheeseman, V. G. Zakrzewski, J. A. Montgomery, Jr., R. E. Stratmann, J. C. Burant, S. Dapprich, J. M. Millam, A. D. Daniels, K. N. Kudin, M. C. Strain, O. Farkas, J. Tomasi, V. Barone, M. Cossi, R. Cammi, B. Mennucci, C. Pomelli, C. Adamo, S. Clifford, J. Ochterski, G. A. Petersson, P. Y. Ayala, Q. Cui, K. Morokuma, D. K. Malick, A. D. Rabuck, K. Raghavachari, J. B. Foresman, J. Cioslowski, J. V. Ortiz, B. B. Stefanov, G. Liu, A. Liashenko, P. Piskorz, I. Komaromi, R. Gomperts, R. L. Martin, D. J. Fox, T. Keith, M. A. Al-Laham, C. Y. Peng, A. Nanayakkara, C. Gonzalez, M. Challacombe, P. M. W. Gill, B. G. Johnson, W. Chen, M. W. Wong, J. L. Andres, M. Head-Gordon, E. S. Replogle and J. A. Pople, GAUSSIAN 98 (Revision A.7), Gaussian, Inc., Pittsburgh, PA, 1998.
- (a) F. Montilla, E. Clara, T. Avilés, T. Casimiro, A. Aguiar Ricardo and M. Nunes da Ponte, *J. Organomet. Chem.*, 2001, **626**(1–2), 227; (b) F. Montilla, T. Avilés, T. Casimiro, A. Aguiar Ricardo and M. Nunes da Ponte, *J. Organomet. Chem.*, 2001, **632**(1–2), 113.
- (a) C. M. Cowey, K. D. Bartle, M. D. Burford, A. A. Clifford, S. Zhu and N. G. Smart, *J. Chem. Eng. Data*, 1995, **40**, 1217; (b) U. Kreher, S. Schebesta and D. Walther, *Z. Anorg. Allg. Chem.*, 1998, **624**, 602.
- E. O. Fischer and R. Jira, *Z. Naturforsch., Teil B*, 1954, **9**, 618.
- M. L. H. Green and G. Wilkinson, *J. Chem. Soc.*, 1958, 4314.
- M. D. Rauch and R. A. Genetti, *J. Org. Chem.*, 1970, **35**, 3888.
- (a) Z. Pang, X.-F. Hou, R.-F. Cai, X.-G. Zhou and Z.-E. Huang, *Synth. React. Inorg. Met.-Org. Chem.*, 2000, **30**, 877; (b) X.-F. Hou, Z. Pang, R.-F. Cai and X.-G. Zhou, *Synth. React. Inorg. Met.-Org. Chem.*, 1998, **28**, 1505.

-
- 26 S. H. Strauss, *J. Chem. Soc., Dalton Trans.*, 2000, 1 and references therein.
- 27 (a) F. Bigoli, P. Deplano, M. L. Mercuri, M. A. Pellinghelli, A. Sabatini, E. F. Trogu and A. Vacca, *J. Chem. Soc., Dalton Trans.*, 1996, 3583; (b) P. Deplano, J. R. Ferraro, M. L. Mercuri and E. F. Trogu, *Coord. Chem. Rev.*, 1999, **188**, 71.
- 28 F. Bigoli, P. Deplano, A. Ienco, C. Mealli, M. L. Mercuri, M. A. Pellinghelli, G. Pintus, G. Saba and E. F. Trogu, *Inorg. Chem.*, 1999, **38**, 4627.
- 29 J. B. Foresman and A. Frisch, in *Exploring Chemistry with Electronic Structure Methods*, Gaussian Inc., Pittsburgh, 1996.
- 30 (a) J. Lupinetti, B. Frenking and S. H. Strauss, *Angew. Chem., Int. Ed.*, 1998, **37**, 2113; (b) J. Lupinetti, V. Jonas, W. Thiel, S. H. Strauss and B. Frenking, *Chem. Eur. J.*, 1999, **5**, 2573.
- 31 (a) F. Loeker and W. Leitner, *Chem. Eur. J.*, 2000, **6**, 2011; (b) G. Musie, W.-M. Wei, B. Subramaniam and D. H. Busch, *Coord. Chem. Rev.*, 2001, **219**, 789.
- 32 R. A. Sheldon and J. K. Kochi, in *Metal-Catalyzed Oxidation of Organic Compounds*, Academic Press, New York, 1981.
- 33 K. A. Jørgensen and B. Schiøtt, *Chem. Rev.*, 1990, **90**, 1483.
- 34 (a) M. K. Trost and R. G. Bergman, *Organometallics*, 1991, **10**, 1172; (b) J. Sundermeyer, *Angew. Chem., Int. Ed. Engl.*, 1993, **32**, 1144.
- 35 C. Reichardt, in *Solvents and Solvent Effects in Organic Chemistry*, VCH, Weinheim, 1988.
- 36 (a) R. Barral, C. Bocard, I. S. Roch and L. Sajus, *Tetrahedron Lett.*, 1972, 1693; (b) R. Durant, C. D. Garner, M. R. Hyde and F. E. Mabbs, *J. Chem. Soc., Dalton Trans.*, 1977, 955.